Open access • Journal Article • DOI:10.1039/B418870E

Dinuclear bis-beta-diketonato ligand derivatives of iron(III) and copper(II) and use of the latter as components for the assembly of extended metallo-supramolecular structures. — Source link

Jack K. Clegg, Leonard F. Lindoy, John C. McMurtrie, John C. McMurtrie ...+1 more authors

Institutions: University of Sydney, Queensland University of Technology

Published on: 21 Feb 2005 - Dalton Transactions (Royal Society of Chemistry)

Topics: Pyrazine, Square pyramidal molecular geometry, Ligand, Crystal engineering and Tautomer

FULL PAPER

Dalton
www.rsc.org/dalton

Dinuclear bis-β-diketonato ligand derivatives of iron(III) and copper(II) and use of the latter as components for the assembly of extended metallo-supramolecular structures†

Jack K. Clegg,[a] Leonard F. Lindoy,*[a] John C. McMurtrie[a,b] and David Schilter[a]

[a] *Centre for Heavy Metals Research, School of Chemistry, University of Sydney, NSW 2006, Australia*

[b] *School of Physical and Chemical Sciences, Queensland University of Technology, GPO Box 2434, Brisbane 4001, Australia*

Received 16th December 2004, Accepted 21st January 2005
First published as an Advance Article on the web 1st February 2005

A range of 1,3-aryl linked, bis-β-diketone derivatives (LH_2) has been employed to synthesise neutral bis(ligand), dinuclear complexes incorporating square-planar copper(II) and tris(ligand) dinuclear helical derivatives containing octahedral iron(III). The ^{1}H NMR spectra of the free ligands contain singlet peaks at *ca.* 16.2 ppm, indicative of enolic protons, confirming that the (bis) enol tautomer is present in solution. An X-ray structure of a ligand from the series incorporating *tert*-butyl terminal substituents confirms that the same tautomer persists in the solid and that the relative orientation of the bis-β-diketone fragments is such that the coordination vectors lie at approximately 120° to each other. The planar, dinuclear copper complexes form 1 : 2 adducts with pyridine and 4-(dimethylamino)pyridine, confirmed by X-ray structures, that incorporate five-coordinate metal centres. Based on this behaviour, the prospect of linking copper centres in the dinuclear complexes using the difunctional heterocyclic bases, 4,4′-bipyridine, 4,4′-*trans*-azopyridine and pyrazine as co-ligands has been probed. However, 4,4′-bipyridine was observed to coordinate through only one of its heterocyclic nitrogen atoms in the solid state to form a 1 : 2 ($[Cu_2(L)_2]$:4,4′-bipyridine) adduct, analogous to the structures obtained with the above mono-functional nitrogen bases. Nevertheless, an X-ray structure determination shows that the related difunctional base, 4,4′-*trans*-azopyridine, coordinates in a bridging fashion *via* both its heterocyclic nitrogen atoms on alternate sides of each planar $[Cu_2(L)_2]$ unit to produce an infinite one dimensional metallo chain. In contrast, with pyrazine, a new neutral, discrete assembly of type $[Cu_4(L)_4(pyrazine)_2]$ is formed. The X-ray structure shows that two planar dinuclear complexes are linked by two pyrazine molecules in a sandwich arrangement such that the coordination environment of each copper ion is approximately square pyramidal with the overall tetranuclear structure thus taking the form of a 'dimer of dimers'.

Introduction

The design and synthesis of discrete metallo assemblies, particularly those with interesting topologies and/or potential technological applications have received much recent attention.[1] For example, in a previous study we described the use of 1,4-aryl-linked, bis-β-diketone derivatives of type **1** as ligands for the construction of uncharged metallo-supramolecular triangles (on interaction with square planar copper(II)) and tetrahedra (on interaction with octahedral iron(III) or gallium(III)).[2] These new species are of stoichiometry $[Cu_3(L)_3]$ and $[M_4(L)_6]$ (M = Fe, Ga), respectively, where LH_2 is a 1,4-aryl linked, bis-β-diketone ligand of type $\mathbf{1}H_2$. The success of this procedure in forming the trinuclear copper species reflects the ability of the β-diketonato fragments to align themselves in a planar fashion such that they are mutually orientated at 60° to each other (see $\mathbf{1}H_2$). Similarly, interaction with the trivalent ions Fe^{3+} and Ga^{3+} generates the above-mentioned tetrahedral species in which the respective bis-β-diketonato ligands form the edges of the tetrahedron, with the metal ions positioned at the corners. In these structures, four of the bis-β-diketonato ligands adopt approximate '*syn*' configurations while two approach '*anti*' arrangements. The tendency to adopt these respective arrangements is undoubtedly a reflection of the presence of conjugated sp^2 carbons in the backbone of each bound ligand.

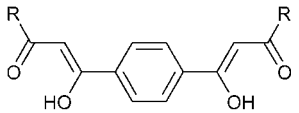

$\mathbf{1}H_2$

The present study has involved the interaction of copper(II) and iron(III) with the related 1,3-aryl linked ligands, $\mathbf{2}H_2$–$\mathbf{5}H_2$ under basic conditions. As mentioned above for ligands of type $\mathbf{1}H_2$, rotation of individual β-diketone fragments about the bonds connecting them to the central aryl rings can occur. For $\mathbf{2}H_2$–$\mathbf{5}H_2$ this gives rise to possible configurations that range from planar 'parallel' β-diketone fragments through to planar fragments that are directed at 120° to each other.

Based on the results of previous studies,[3,4] it was anticipated that metal coordination by pairs of bis-β-diketonato ligands (chosen from $\mathbf{2}H_2$–$\mathbf{5}H_2$) would occur in their 'parallel' configurations to two copper ions to yield discrete, planar (dinuclear) complexes. Indeed, such a geometry was assigned from physical measurements to the neutral copper complex of 2 : 2 (Cu^{2+}: $(\mathbf{2})^{2-}$) stoichiometry, where $\mathbf{2}^{2-}$ is the doubly deprotonated derivative of $\mathbf{2}H_2$.[3] On reaction with trivalent, octahedral metals, neutral triple helical complexes of type $M_2(L)_3$ were similarly anticipated;[4,5] since such a geometry has been assigned previously to related complexes incorporating the doubly deprotonated form of **6** with M = vanadium(III), manganese(III) or iron(III).[5] In this latter study the helical structure of the manganese(III) complex was confirmed by X-ray diffraction. It is also noted that, more recently, $\mathbf{6}H_2$ (as well as its ethoxy-substituted aryl derivative) has been demonstrated

† Electronic supplementary information (ESI) available: Individual crystal structure refinement details. See http://www.rsc.org/suppdata/dt/b4/b418870e/

DOI: 10.1039/b418870e

to form dinuclear, tri-stranded complexes of type $[M_2(\mathbf{6})_3]$ with a selection of trivalent lanthanide ions.[6] Aspects of the metal ion chemistry of related ligand species incorporating additional donors in, or attached to, the central aromatic spacer have also been reported.[7]

We now report the synthesis of new examples of neutral, dinuclear copper(II) and iron(III) complexes incorporating doubly deprotonated ligands chosen from $\mathbf{2}H_2$–$\mathbf{5}H_2$. Of particular interest was the potential for further coordination at the metal centres in the dinuclear copper complexes to produce extended supramolecular entities.

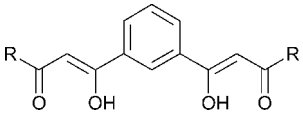

$\mathbf{2}H_2$; R = Me
$\mathbf{3}H_2$; R = Et
$\mathbf{4}H_2$; R = Pr
$\mathbf{5}H_2$; R = ^{t}Bu
$\mathbf{6}H_2$; R = Ph

Experimental

All reagents were purchased from commercial sources and used without further purification. Tetrahydrofuran and diethyl ether were dried over sodium wire. ^{1}H NMR spectra were recorded on a Bruker Avance DPX200 spectrometer; δH values are relative to tetramethylsilane. Low resolution electrospray ionisation mass spectra (ESI-MS) were obtained on a Finnigan LCQ-8 spectrometer. UV-vis spectra were recorded on a Cary 1E spectrophotometer in the solid state and FTIR (KBr) spectra were collected using a Bio-Rad FTS-40 spectrometer. All products were dried over P_4O_{10} in a vacuum before microanalysis.

Ligand and metal complex synthesis

Synthesis of $\mathbf{2}H_2$–$\mathbf{5}H_2$. This was based on previously reported procedures.[8] To a mixture of dimethyl-isophthalate (5 g, 0.025 mol) (for $\mathbf{2}H_2$–$\mathbf{5}H_2$) and acetone (2.9 g, 0.05 mol) (for $\mathbf{2}H_2$), butan-2-one (3.6 g, 0.05 mol) (for $\mathbf{3}H_2$), pentan-2-one (4.3 g, 0.05 mol) (for $\mathbf{4}H_2$), 3,3-dimethylbutan-2-one (5 g, 0.05 mol) (for $\mathbf{5}H_2$), in dry diethyl ether (80 ml) was added sodium amide (5 g, 0.13 mol) at 0 °C. In each case the mixture was stirred for 2 h at this temperature and then 2 h at room temperature during which time the reaction mixture turned yellow. The mixture was quenched with iced water (100 ml), and the aqueous layer was separated and acidified with CO_2(s) to yield an off-white precipitate that was collected by filtration. The ether layer was allowed to evaporate and the off-white residue that remained was combined with the above precipitate; the mixture was recrystallised from methanol.

1,1′-(1,3-Phenylene)-bis-butane-1,3-dione 0.25 hydrate $\mathbf{2}H_2$. Yield 2.8 g (46%); pale yellow/orange needles. Found: C, 66.85; H, 5.79. Calc. for $C_{14}H_{14}O_4.0.25H_2O$: C, 67.04; H, 5.83%. ^{1}H NMR δ (200 MHz, $CDCl_3$): 16.01 (br, s, –OH, 2H), 8.36 (s, aromatic, H), 8.04 (dd, aromatic, 2H), 7.55 (t, aromatic, H), 6.24 (s, H_γ, 2H), 2.22 ppm (s, $-CH_3$, 6H). ESI-MS *m/z*: 247 $\{M + H\}^+$. FTIR (KBr): 3000 (br), 2362, 2339, 1600 (vbr), 1483, 1202, 1087, 996, 960, 786 cm^{-1}.

1,1′-(1,3-Phenylene)-bis-pentane-1,3-dione $\mathbf{3}H_2$. Yield 3.2 g (47%); pale orange needles. Found: C, 69.86; H, 6.80. Calc. for $C_{16}H_{18}O_4$: C, 70.06; H, 6.61%. ^{1}H NMR δ (200 MHz $CDCl_3$): 16.08 (br, *s*, –OH, 2H), 8.36 (s, aromatic, H), 8.04 (dd, aromatic, 2H), 7.55 (t, aromatic, H), 6.24 (*s*, H_γ, 2H), 2.52 (q, $-CH_2-$, 4H), 1.23 ppm (t, $-CH_3$, 6H). ESI-MS *m/z*: 275 $\{M + H\}^+$, 297 $\{M + Na\}^+$. FTIR (KBr): 3000 (br), 1600 (vbr), 1484, 1381, 1319, 1283, 1244, 1104, 1086, 1003, 932, 883, 773 cm^{-1}.

1,1′-(1,3-Phenylene)-bis-hexane-1,3-dione $\mathbf{4}H_2$. Yield 3.3 g (44%); pale orange needles. Found: C, 71.57; H, 7.45. Calc. for $C_{18}H_{22}O_4$: C, 71.50; H, 7.33%. ^{1}H NMR δ (200 MHz $CDCl_3$): 16.16 (br, s, enol, 2H), 8.36 (s, aromatic, H), 8.04 (dd, aromatic, 2H), 7.55 (t, aromatic, H), 6.23 (s, H_γ, 2H), 2.48 (t, CH_2, 4H), 1.72 (q, CH_2, 4H), 1.02 ppm (t, CH_3, 6H). ESI-MS *m/z*: 303 $\{M + H\}^+$, 325 $\{M + Na\}^+$. FTIR (KBr): 2890 (br), 1600 (vbr), 1559, 1507, 1472, 1457, 1362, 1298, 1238, 1191, 1154, 1073, 951, 775, 747, 693 cm^{-1}.

1,1′-(1,3-Phenylene)-bis-4,4-dimethylpentane-1,3-dione $\mathbf{5}H_2$. Yield 2.6 g (32%); colourless needles. Found: C, 72.43; H, 8.11. Calc. for $C_{20}H_{26}O_4$: C, 72.70; H, 7.93%. ^{1}H NMR δ (200 MHz $CDCl_3$): 16.40 (br, s, enol, 2H), 8.38 (s, aromatic, H), 8.04 (dd, aromatic, 2H), 7.55 (t, aromatic, H), 6.34 (s, H_γ, 2H), 1.27 ppm (s, CH_3,18H). ESI-MS *m/z*: 331 $\{M + H\}^+$, 353 $\{M + Na\}^+$. FTIR (KBr): 3000 (br), 1600 (vbr), 1559, 1480, 1465, 1430, 1363, 1310, 1288, 1226, 1166, 1135, 11093, 1018, 940, 877, 805, 704, 647 cm^{-1}. The crystals used for X-ray crystallography were obtained by slow evaporation of a diethyl ether solution of this product.

Complexes of type $[Cu_2(L)_2]$ (L = 2–5) and $[Fe_2(L)_3]$ (L = 2, 5). The required ligand (0.002 mol) (chosen from **2**–**5**) in dry THF (40 ml) was added to $NaHCO_3$ (1.0 g, 0.008 mol) or Na_2CO_3 (1.0 g, 0.01 mol) in dry THF (10 ml). The mixture was stirred for 1 h before copper(II) chloride dihydrate (0.002 mol), or anhydrous iron(III) chloride (0.0013 mol) dissolved in dry THF (40 ml) was added dropwise. The respective mixtures were stirred for a further 2 h and filtered. The filtrate was either allowed to evaporate slowly to yield the solid complex which was isolated by filtration; alternatively, the solvent was removed on a rotary evaporator and the crude solid so obtained was recrystallised from THF. All products were washed with methanol before microanalysis.

*[Cu$_2$(**2**)$_2$]·2.5THF.* Yield 0.41 g (52%); green microcrystalline powder. Found: C, 57.68; H, 5.83; N: 0.13. Calc. for $C_{28}H_{24}Cu_2O_8{\cdot}2.5(C_4H_8O)$: C, 57.35; H, 5.57%. UV-vis (solid state): 550 (sh), 710 (br) nm.

*[Cu$_2$(**3**)$_2$].* Yield 0.44 g (65%); green microcrystalline powder. Found: C, 57.32; H, 5.00. Calc. for $C_{32}H_{32}Cu_2O_8$: C, 57.22; H, 4.80%. UV-vis (solid state): 555 (sh), 685 (br) nm.

*[Cu$_2$(**4**)$_2$]·H$_2$O.* Yield 0.39 g (52%); green microcrystalline powder. Found: C, 58.19; H, 5.66. Calc. for $C_{36}H_{40}Cu_2O_8{\cdot}H_2O$: C, 58.05; H, 5.69.%. ESI-MS (*m/z*): 1677 $\{2M + Ag\}^+$, 892 $\{M + Ag\}^+$. UV-vis (solid state): 550 (sh), 660 (br) nm.

*[Cu$_2$(**5**)$_2$(THF)$_2$].* Yield 0.7 g (74%); green microcrystalline powder. Found: C, 62.36; H, 7.07. Calc. for $C_{40}H_{48}Cu_2O_8{\cdot}2(C_4H_8O)$: C, 62.12; H, 6.95%. UV-vis (solid state): 530 (sh), 680 (br) nm. Evaporation of a THF solution of the product from a partially sealed container over several months yielded crystals suitable for X-ray structure analysis.

*[Fe$_2$(**2**)$_3$]·5H$_2$O.* Yield 0.37 g (54%); red microcrystalline powder. Found: C, 53.64; H, 4.49. Calc. for $C_{42}H_{36}Fe_2O_{12}{\cdot}5H_2O$: C, 53.98; H, 4.96%. UV-vis (solid state): 460 (sh) nm.

*[Fe$_2$(**5**)$_3$]·7H$_2$O.* Yield 0.41 g (50%); red crystals. Found: C, 59.22; H, 6.73. Calc. for $C_{60}H_{72}Fe_2O_{12}{\cdot}7H_2O$: C, 58.92; H, 7.03%. UV-vis (solid state): 460 sh nm. Crystals suitable for the X-ray diffraction study were obtained by slow diffusion of ether vapour into the filtrate obtained from the preparation of $[Fe_2(\mathbf{5})_3]{\cdot}7H_2O$—see general synthetic procedure given earlier.

Pyridine (py), 4-(dimethylamino)pyridine (dmapy), 4,4′-bipyridine (bipy), 4,4′-*trans*-azopyridine (azpy) and pyrazine (pyz) adducts.

*[Cu$_2$(**5**)$_2$(py)$_2$]·py.* Pyridine (0.079 g, 1.0 mmol) was added to a solution of $[Cu_2(\mathbf{5})_2(THF)_2]$ (0.46 g, 0.50 mmol) in THF (40 ml). The resulting dark green solution was stirred for 1 h during which time the colour changed slightly to bright green. Crystals of $[Cu_2(\mathbf{5})_2(py)_2]{\cdot}py$ were obtained upon evaporation of the THF solution over a period of 1 week and a crystal from

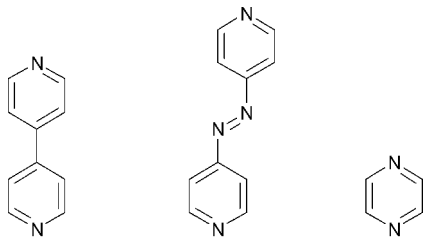

bipy azpy pyz

this crop was used for an X-ray structure determination. On removal from the mother liquor the complex rapidly loses both the pyridine solvate as well as each of the coordinated pyridines. The elemental analysis of a vacuum dried sample of this product corresponded to the fully desolvated parent complex, $[Cu_2(\mathbf{5})_2]$. Found C, 61.29; H, 6.33; N, 0. Calc. for $C_{40}H_{48}Cu_2O_8$: C, 61.29; H, 6.17; N, 0%.

[Cu₂(5)₂(dmapy)₂]·0.5THF. A stirred solution of $[Cu_2(\mathbf{5})_2(THF)_2]$ (0.26 mmol) and 4-(dimethylamino)pyridine (0.52 mmol) in THF (25 ml) was heated until boiling then allowed to cool. Slow evaporation of the reaction mixture afforded $[Cu_2(\mathbf{5})_2(dmapy)_2]\cdot 0.5THF$ as green crystals, one of which was used for an X-ray structure determination. Yield 0.258 g (91%). Found: C, 63.45; H, 6.77; N, 5.32. Calc. for $C_{56}H_{72}Cu_2N_4O_{8.5}$: C, 63.20; H, 6.82; N, 5.26%. *m/z* (ESI-MS) (Ag^+ added to sample): 1014 $(M–dmapy + Ag)^+$. UV-Vis (solid state): 425 (sh), 670 (br), nm. FTIR (KBr): 2961, 1603, 1593, 1565, 1523, 1502, 1478, 1417, 1226, 1002, 775 cm^{-1}.

[Cu₂(5)₂(bipy)₂]·2bipy. A stirred solution of $[Cu_2(\mathbf{5})_2(THF)_2]$ (0.052 g, 0.060 mmol) and 4,4′-bipyridine (0.050 g, 0.32 mmol) in THF (25 ml) was briefly brought to reflux and then allowed to cool to room temperature. Slow evaporation of solvent from the reaction mixture afforded small olive green crystals of $[Cu_2(\mathbf{5})_2(bipy)_2]\cdot 2bipy$, one of which was used for an X-ray structure determination. Yield 0.056 g (66%). UV-vis (solid state): 435 (sh), 640 (br) nm. FTIR (KBr): 654, 678, 710, 780, 889, 988, 1084, 1157, 1215, 1300, 1412, 1480, 1498, 1313, 1550, 1567, 2964, 2980 cm^{-1}.

[Cu₂(5)₂(azpy)]ₙ·(2THF)ₙ. A stirred solution of $[Cu_2(\mathbf{5})_2(THF)_2]$ (0.092 g, 0.10 mmol) and 4,4′-*trans*-azopyridine (0.018 g, 0.10 mmol) in THF (25 ml) was brought to reflux and then allowed to cool to room temperature. Slow evaporation of the reaction mixture afforded $[Cu_2(\mathbf{5})_2(azpy)]_n\cdot(2THF)_n$ as large green/orange dichroic crystals, one of which was employed for X-ray analysis. The sample was dried over anhydrous P_2O_5 prior to elemental analysis. Yield 0.90 g (80%). Found: C, 62.21; H, 6.51; N, 4.42. Calc. for $C_{58}H_{72}Cu_2N_4O_{10}$: C, 62.63; H, 6.52; N, 5.04%. UV-vis (solid state): 475 (sh), 680 (br) nm. FTIR (KBr): 706, 774, 840, 955, 1223, 1296, 1359, 1406, 1415, 1479, 1537, 1590 cm^{-1}.

[Cu₄(5)₄(pyz)₂]·4THF. A stirred solution of $[Cu_2(\mathbf{5})_2(THF)_2]$ (0.092 g, 0.10 mmol) and pyrazine (0.040 g, 0.50 mmol) in THF (25 ml) was brought to reflux and then allowed to cool to room temperature. Slow evaporation of solvent from the reaction mixture afforded a very small quantity of small green crystals, one of which was employed for an X-ray structure determination without full characterisation. Yield 0.011 g (13%). UV-vis (solid state): 445(sh), 675 (br) nm.

X-Ray structure determinations

Data were collected at 150(2) K with ω scans to approximately 56° 2θ using a Bruker SMART 1000 diffractometer employing graphite-monochromated Mo-Kα radiation generated from a sealed tube (0.71073 Å). Data integration and reduction were undertaken with SAINT and XPREP[9] and subsequent computations were carried out using the WinGX-32 graphical user interface.[10] Multi-scan empirical absorption corrections were applied to the data using the program SADABS.[11] The structures were solved by direct methods using SIR97[12] then refined and extended with SHELXL-97.[13] In general, ordered non-hydrogen atoms with occupancies greater than or equal to 0.5 were refined anisotropically. Partial occupancy carbon, nitrogen and oxygen atoms were refined isotropically. Carbon-bound hydrogen atoms were included in idealised positions and refined using a riding model. Oxygen-bound hydrogen atoms that were structurally evident in the difference Fourier map were included and refined with bond length and angle restraints.

Crystal data

Crystal and structure refinement data for ligand $\mathbf{5}H_2$, $[Fe_2(\mathbf{5})_3]\cdot Et_2O$, $[Cu_2(\mathbf{5})_2(THF)_2]$, $[Cu_2(\mathbf{5})_2(py)_2]\cdot py$, $[Cu_2(\mathbf{5})_2(dmapy)_2]\cdot 3.25THF$, $[Cu_2(\mathbf{5})_2(bipy)_2]\cdot 2bipy$, $[Cu_2(\mathbf{5})_2(azpy)_2]\cdot 2THF$ and $[Cu_4(\mathbf{5})_4(pyz)_2]\cdot 4THF$ are summarised in Tables 1–3. ORTEP[14] depictions of the crystal structures are provided in Figs. 1–6 and S1 and S2 in the ESI†. Where applicable, additional details relating to the X-ray crystal structure (along with tables of selected bond lengths and angles) are given in the ESI†.

Specific details for $[Cu_2(\mathbf{5})_2(dmapy)_2]\cdot 3.25THF$. While the solvated crystal employed appeared quite stable at 150 K, there was some loss of crystal quality during the mounting process (prior to quenching at 150 K), despite rapid handling at low temperature (*ca.* 1 min at 200 K). The final difference Fourier map contained two residual electron density peaks of significant size (2.96 e^- $Å^{-3}$ peak 1.92 Å from N(4) and 2.81 e^- $Å^{-3}$ peak 2.41 Å from C(11)). Due to their proximity to the main residue neither of these can be plausibly modelled and both are likely to be artifacts resulting from crystal deterioration during the mounting process. Idealised intramolecular atom–atom distance restraints were applied to the THF solvent molecules comprising atoms O(3T), C(9T)–C(12T) and O(4T), C(13T)–C(16T) and to the disordered ᵗBu groups comprising atoms C(1)–C(5) (positions A and B) and C(16)–C(20) (positions A and B) to facilitate refinement with a realistic molecular model (see ESI†, Fig. S1).

Table 1 Crystal and structure refinement data for ligand $\mathbf{5}H_2$ and $[Fe_2(\mathbf{5})_3]\cdot Et_2O$

	$\mathbf{5}H_2$	$[Fe_2(\mathbf{5})_3]\cdot Et_2O$
Formula	$C_{20}H_{26}O_4$	$C_{64}H_{82}Fe_2O_{13}$
M	330.41	1171.0
Crystal system	Monoclinic	Monoclinic
Space group	*C*2/*c* (#15)	$P2_1/c$ (#14)
a/Å	19.3711(10)	17.6982(15)
b/Å	9.5415(5)	19.0959(16)
c/Å	10.8882(6)	20.1570(17)
α/°		
β/°	116.1840(17)	111.6490(10)
γ/°		
V/Å³	1805.94(17)	6331.8(9)
D_c/g cm^{-3}	1.215	1.228
Z	4	4
Size/mm	0.55 × 0.44 × 0.29	0.49 × 0.45 × 0.18
Colour	Colourless	Orange
Habit	Prism	Prism
μ(Mo-Kα)/mm^{-1}	0.083	0.517
$T_{min,max}$	0.864, 0.980	0.740, 0.913
$2\theta_{max}$/°	56.6	56.6
hkl Range	−25 to 25	−23 to 23
	−12 to 12	−25 to 25
	−14 to 14	−26 to 26
N	8673	61704
N_{ind} (R_{merge})	2176 (0.0147)	15183 (0.0414)
N_{obs} ($I > 2\sigma(I)$)	1972	11008
N_{var}	116	730
$R1^a$ (F, 2σ)	0.0402	0.0450
$wR2^a$ (F^2, all)	0.1170	0.1334
A^a, B^a	0.0658, 1.013	0.0732, 2.841
GoF (all)	1.054	1.023
$\Delta\rho_{min,max}$/e^- $Å^{-3}$	−0.228, 0.350	−0.516, 0.726

Table 2 Crystal and structure refinement data for $[Cu_2(\mathbf{5})_2(THF)_2]$, $[Cu_2(\mathbf{5})_2(py)_2]\cdot py$ and $[Cu_2(\mathbf{5})_2(dmapy)_2]\cdot 3.25THF$

	$[Cu_2(\mathbf{5})_2(THF)_2]$	$[Cu_2(\mathbf{5})_2(py)_2]\cdot py$	$[Cu_2(\mathbf{5})_2(dmapy)_2]\cdot 3.25THF$
Formula	$C_{48}H_{64}Cu_2O_{10}$	$C_{55}H_{63}Cu_2N_3O_8$	$C_{67}H_{94}Cu_2N_4O_{11.25}$
M	928.07	1021.16	1262.54
Crystal system	Triclinic	Triclinic	Triclinic
Space group	$P\bar{1}$ (#2)	$P\bar{1}$ (#2)	$P\bar{1}$ (#2)
a/Å	7.0109(7)	8.4084(16)	14.900(3)
b/Å	10.5767(11)	10.0249(19)	15.948(3)
c/Å	16.5539(17)	17.246(3)	17.283(3)
α/°	95.966(2)	97.396(3)	94.774(3)
β/°	95.216(2)	99.356(3)	107.625(3)
γ/°	104.527(2)	110.158(3)	111.025(3)
V/Å^3	1173.1(2)	1319.5(4)	3567.5(12)
D_c/g cm^{-3}	1.314	1.285	1.175
Z	1	1	2
Size/mm	0.42 × 0.32 × 0.17	0.49 × 0.20 × 0.07	0.55 × 0.21 × 0.08
Colour	Intense blue	Green	Green
Habit	Prism	Prism	Prism
μ(Mo-Kα)/mm^{-1}	0.961	0.860	0.652
$T_{min,max}$	0.724, 0.849	0.782, 0.942	0.668, 0.949
$2\theta_{max}$/°	56.6	56.7	56.6
hkl Range	−9 to 9	−11 to 11	−19 to 19
	−14 to 13	−13 to 13	−21 to 21
	−22 to 22	−22 to 22	−22 to 22
N	11339	12746	33366
N_{ind} (R_{merge})	5382 (0.0166)	6069 (0.0230)	16053 (0.0445)
N_{obs} ($I > 2\sigma(I)$)	4840	5038	10407
N_{var}	277	313	759
$R1^a$ (F, 2σ)	0.0286	0.0375	0.0813
$wR2^a$ (F^2, all)	0.0789	0.1024	0.2440
A^a, B^a	0.0439, 0.3992	0.0625, 0.1906	0.139, 3.53
GoF (all)	1.052	1.043	1.043
$\Delta\rho_{min,max}$/e$^-$ Å^{-3}	−0.563, 0.529	−0.618, 0.714	−0.663, 2.960

^{a} $R1 = \Sigma\|F_o| - |F_c\|/\Sigma|F_o|$ for $F_o > 2\sigma(F_o)$ and $wR2 = \{\Sigma[w(F_o^2 - F_c^2)^2]/\Sigma[w(F_c^2)^2]\}^{1/2}$ where $w = 1/[\sigma^2(F_o^2) + (AP)^2 + BP]$, $P = (F_o^2 + 2F_c^2)/3$.

Table 3 Crystal and structure refinement data for $[Cu_2(\mathbf{5})_2(bipy)_2]\cdot 2bipy$, $[Cu_2(\mathbf{5})_2(azpy)_2]\cdot 2THF$ and $[Cu_4(\mathbf{5})_4(pyz)_2]\cdot 4THF$

	$[Cu_2(\mathbf{5})_2(bipy)_2]\cdot 2bipy$	$[Cu_2(\mathbf{5})_2(azpy)]\cdot 2THF$	$[Cu_4(\mathbf{5})_4(pyz)_2]\cdot 4THF$
Formula	$C_{80}H_{80}Cu_2N_8O_8$	$C_{55}H_{72}Cu_2N_4O_{10}$	$C_{104}H_{136}Cu_4N_4O_{20}$
M	1408.60	1112.28	2016.33
Crystal system	Monoclinic	Triclinic	Monoclinic
Space group	$P2_1/c$	$P\bar{1}$ (#2)	$C2/c$
a/Å	11.8449(7)	10.426(4)	37.359(3)
b/Å	11.7625(7)	16.570(7)	14.9784(10)
c/Å	25.3454(15)	17638(7)	20.4038(14)
α/°		110.476(6)	
β/°	94.3280(10)	92.635(7)	116.9050(10)
γ/°		100.853(6)	
V/Å^3	3521.2(4)	2783(2)	10181.7(12)
D_c/g cm^{-3}	1.329	1.328	1.315
Z	2	2	4
Size/mm	0.54 × 0.54 × 0.25	0.37 × 0.34 × 0.23	0.59 × 0.53 × 0.23
Colour	Green	Green	Green
Habit	Prism	Prism	Prism
μ(Mo-Kα)/mm^{-1}	0.667	0.825	0.893
$T_{min,max}$	0.760, 0.846	No correction	0.625, 0.814
$2\theta_{max}$/°	56.6	56.6	56.6
hkl Range	−15 to 15	−13 to 13	−49 to 49
	−15 to 15	−21 to 21	−19 to 19
	−32 to −32	−22 to 22	−27 to 27
N	33963	21930	48373
N_{ind} (R_{merge})	8407 (0.0209)	12117 (0.1249)	12117 (0.0448)
N_{obs} ($I > 2\sigma(I)$)	7108	4984	8629
N_{var}	448	655	607
$R1^a$ (F, 2σ)	0.0422	0.1061	0.0425
$wR2^a$ (F^2, all)	0.1247	0.3360	0.1160
A^a, B^a	0.0705, 2.2948	0.1766, 0.0	0.0562, 13.339
GoF (all)	1.048	0.966	1.012
$\Delta\rho_{min,max}$/e$^-$ Å^{-3}	−0.467, 0.979	3.338, −1.233	−0.521, 1.053

^{a} $R1 = \Sigma\|F_o| - |F_c\|/\Sigma|F_o|$ for $F_o > 2\sigma(F_o)$ and $wR2 = \{\Sigma[w(F_o^2 - F_c^2)^2]/\Sigma[w(F_c^2)^2]\}^{1/2}$ where $w = 1/[\sigma^2(F_o^2) + (AP)^2 + BP]$, $P = (F_o^2 + 2F_c^2)/3$.

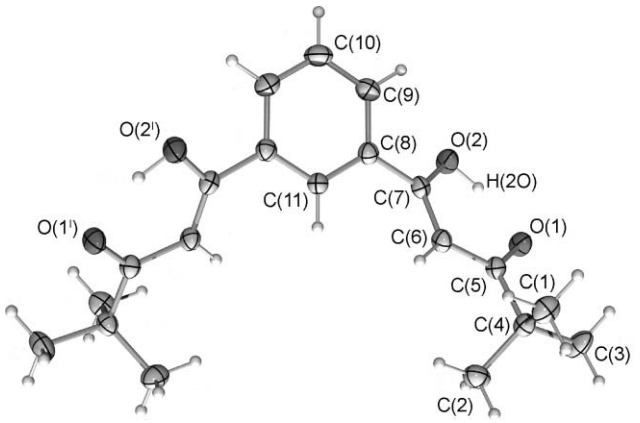

Fig. 1 ORTEP representation of the structure of $\mathbf{5}H_2$ (1,1′-(1,3-phenylene)-bis-4,4-dimethylpentane-1,3-dione). The molecule occupies a crystallographic 2-fold site (symmetry code; $1 - x + 2$, y, $-z + \frac{1}{2}$). The β-diketone groups are in their enol form with the enolic proton attached to O(2) (the oxygen atom nearest the central benzene ring) and there is an intramolecular hydrogen bond typical of enolic β-diketones (O(2)···O(1) distance 2.504(1) Å; O(2)-H(2O)-O(1) angle 153(2)°). Thermal ellipsoids are drawn at the 50% probability level.

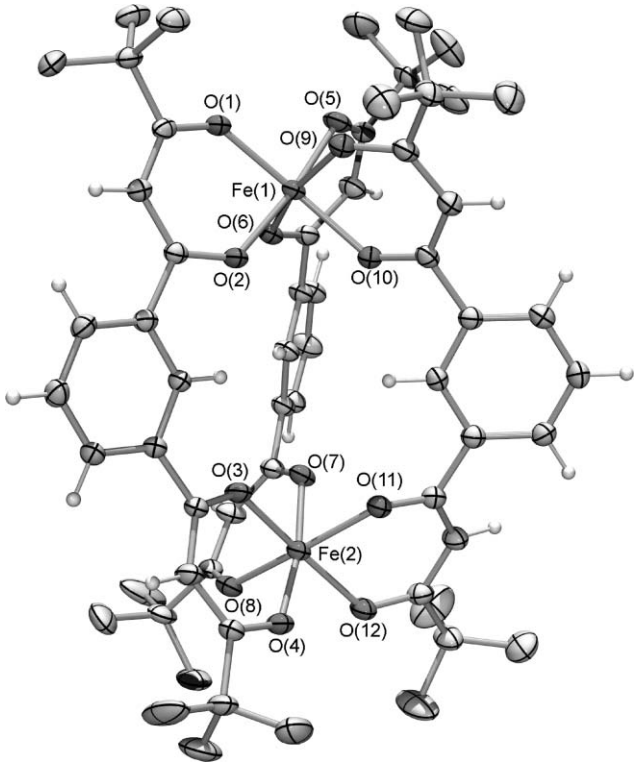

Fig. 2 ORTEP representation of the triple helicate $[Fe_2(\mathbf{5})_3]\cdot Et_2O$ (*t*-butyl hydrogen atoms and ether solvate omitted), 50% probability ellipsoids.

Specific details for [Cu(5)$_2$(azpy)]·2THF. The crystals of this complex displayed very poor diffraction properties. Few reflections at high angles were obtained and the diffraction was very broad. This was despite the fact that the crystals appeared (at least visually) to be well formed and unblemished by fissures. Data were collected on several different crystals from two different batches, however, all displayed equally poor diffraction. The poor quality of the crystal structure—*i.e.* moderately inconsistent temperature factors, relatively low bond precision, high electron density residual peaks (3.338 e^- Å^{-3}) and high *R* factors—reflects the poor diffraction properties of the crystals. The diffraction data also displayed indications of non-merohedral twinning in all of the crystals employed. Attempts to resolve this twinning using GEMINI[9] were unsuccessful. Given the possibility of non-merohedral twinning, no absorption corrections were applied to the data. Atom–atom distance restraints were applied to the disordered THF molecules comprising O(2T), C(5T)–C(8T) and O(3T), C(9T)–C(12T) and to the pyridine rings of the azopyridine ligands comprising N(1), C(41)–C(45) (positions A and B) and N(4), C(46)–C(50) (see ESI†, Fig. S2). In order to achieve least-squares convergence and to obtain sensible (albeit large) temperature factors, global isotropic restraints were applied for the refinement of anisotropic thermal parameters.

Where applicable, additional details relating to the X-ray structures (along with tables of selected bond lengths and angles) are given in the ESI†.

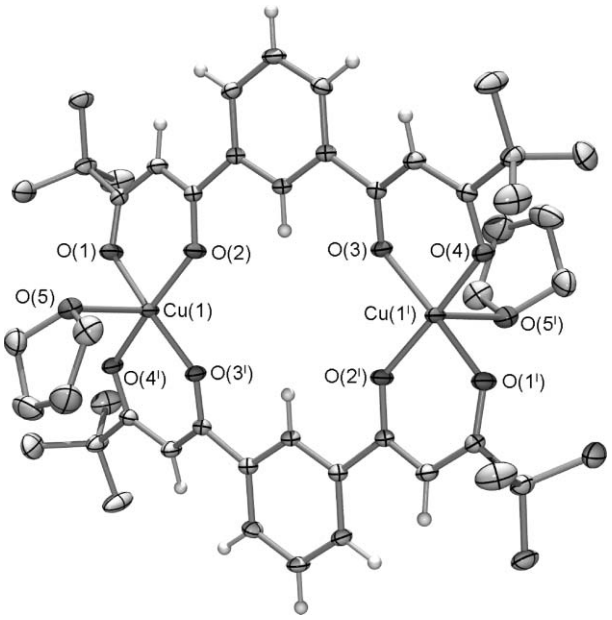

Fig. 3 ORTEP depiction of $[Cu_2(\mathbf{5})_2(THF)_2]$ with 50% probability ellipsoids (*t*-butyl hydrogen atoms omitted). The complex has crystallographic inversion symmetry (symmetry code: $^1 - x, -y, -z$).

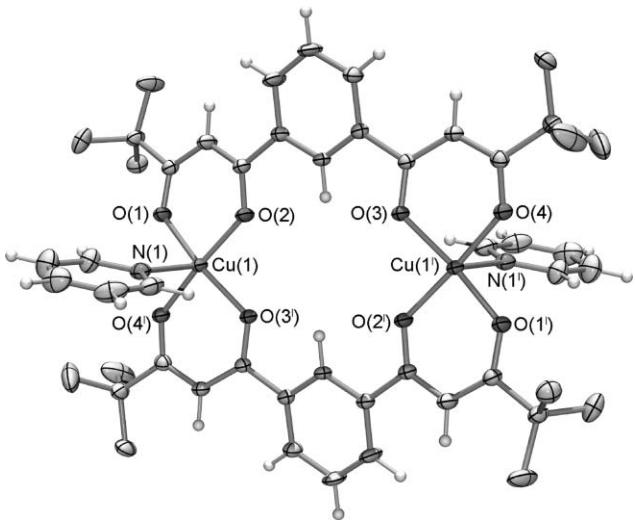

Fig. 4 ORTEP depiction of $[Cu_2(\mathbf{5})_2(py)_2]\cdot py$ (*t*-butyl hydrogen atoms and pyridine solvate omitted). The complex has crystallographic inversion symmetry (symmetry code: $^1 - x, -y, -z$). Thermal ellipsoids are drawn at the 50% probability level.

Results and discussion

The syntheses of $\mathbf{2}H_2$–$\mathbf{5}H_2$ involved Claisen condensations using an adaptation of literature procedures.[8] The ^{1}H NMR spectra of a deuterochloroform solution in each case indicated that these species exist almost entirely in their (bis) enol tautomeric forms, as evidenced by the presence of a broad resonance

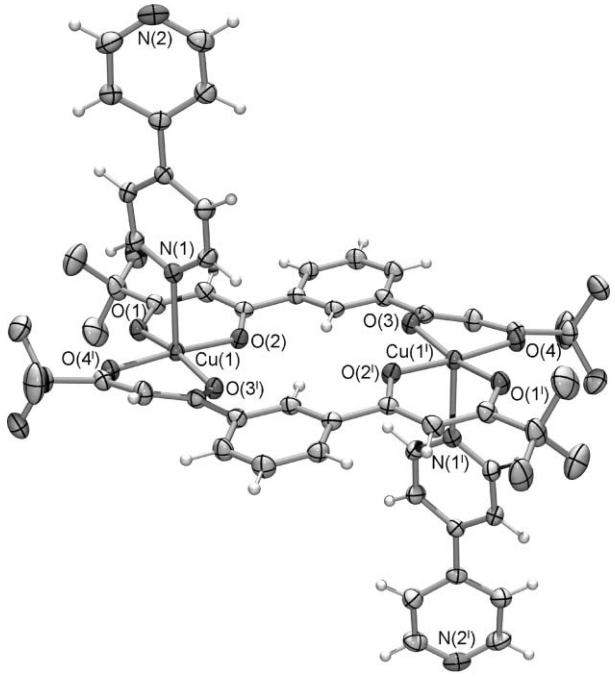

Fig. 5 An ORTEP representation of $[Cu_2(\mathbf{5})_2(bipy)_2]\cdot 2bipy$ (*t*-butyl-hydrogen atoms and 4,4′-bipyridine co-crystallates not shown), ellipsoids are drawn at 50% probability. The complex displays crystallographic inversion symmetry (symmetry code: $^{I} -x, -y, -z+1$).

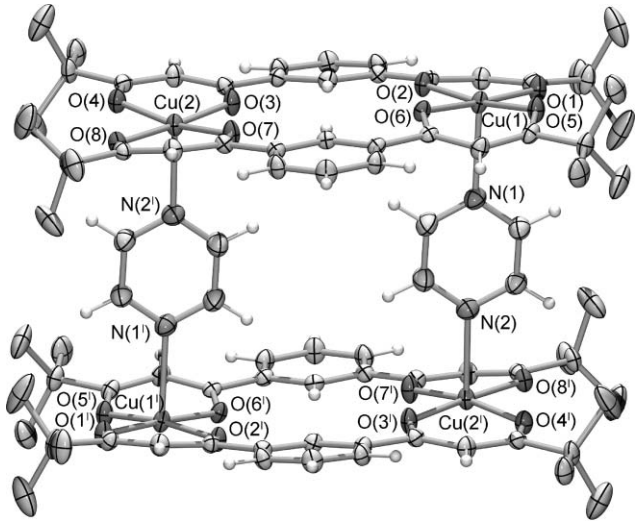

Fig. 6 An ORTEP representation of the tetranuclear structure of $[Cu_4(\mathbf{5})_4(pyz)_2]\cdot 4THF$ (*t*-butyl hydrogen atoms and THF solvates omitted), thermal ellipsoids are drawn at 50% probability. Two dinuclear planar copper(II) complexes are bridged by two difunctional pyrazine ligands and the complex displays crystallographic inversion symmetry (symmetry code: $^{I} -x+1/2, -y+1/2, -z+1$).

at ~16.2 ppm (enol protons), integrating to two protons, in the respective spectra. The existence of a sharp singlet, also integrating to two protons, in each spectrum at ~6.2 ppm (due to H_γ) is also in accord with this assignment. Furthermore, in the solid state, the infrared spectra show absorptions at ~3000 and ~1600 cm^{-1}, suggesting the presence of hydrogen bonded hydroxyl and carbonyl groups, respectively.[15] The occurrence of O–H···O hydrogen bonding in the (bis) enol form of β-diketones, as well as the conjugated nature of this tautomer confers added stability on the structure with respect to its corresponding (bis) keto form.[16]

In relation to the above, it was of interest to investigate what arrangement the present ligands might adopt in the solid state with respect to the enol/keto tautomerism possible but also in terms of the preferred relative orientations adopted by the β-diketone fragments. The X-ray structure of $\mathbf{5}H_2$ (Fig. 1) shows that the β-diketone groups, which are both present in their enol form, are aligned such that their coordination vectors are directed at approximately 120° with respect to each other.

Dinuclear iron(III) and copper(II) complexes

The interaction of iron(III) with the 1,3-aryl bridged bis-β-diketones, $\mathbf{2}H_2$ and $\mathbf{5}H_2$, under basic conditions, yielded neutral dinuclear species of type $[Fe_2(L)_3]\cdot n$(solvent) in each case. These products gave UV-vis spectra that are similar to those of simple tris(β-diketonato)iron(III) complexes.[17] The X-ray structure of $[Fe_2(\mathbf{5})_3]\cdot Et_2O$ has been determined (Fig. 2). The two iron(III) centres are bridged by three ligands to produce a triple helical arrangement in which each iron(III) is surrounded by three β-diketonato fragments so that coordination saturation is achieved. Each dinuclear complex has homochiral iron(III) centres (either Λ–Λ or Δ–Δ). The space group is $P21/c$ which contains inversion centres, therefore each crystal has equal numbers of Λ–Λ and Δ–Δ complexes in it.

As mentioned earlier, there are now several examples in which these and related difunctional ligands (incorporating 'parallel' donor moieties) produce dinuclear triple helicates upon coordination to a trivalent metal ion.[5,18]

Dinuclear copper species of type $Cu_2(L)_2\cdot n$(solvent) were synthesised by reaction of a 1 : 1 ratio of ligand to copper(II) chloride in THF in the presence of base. The UV-vis spectra of the copper(II) complexes are listed in the Experimental section. All spectra consist of a broad envelope of d–d bands (two λ_{max} being evident) in the visible region together with more intense peaks in the UV region corresponding to charge transfer/ligand bands. The spectra are quite similar to those reported previously for 'simple' β-diketone complexes of type [Cu(β-diketonato)$_2$].[19]

The X-ray structure of $[Cu_2(\mathbf{5})_2(THF)_2]$ is presented in Fig. 3. This discrete dinuclear complex has two copper(II) ions bridged by two **5** ligands in a planar arrangement. Each copper(II) centre is 5-coordinate with an approximate square pyramidal geometry. Four β-diketonato oxygen atoms coordinate in the basal plane to each copper with an apical position being occupied by a THF molecule. The THF molecules protrude on opposite sides of the mean plane of the $Cu_2(\mathbf{5})_2$ component.

Monodentate base adducts of $Cu_2(5)_2$

In our previous study we showed that the copper(II) centres in complexes containing the 1,4-aryl linked ligands of type **1** prefer either 4-coordinate square planar coordination involving two β-diketonato fragments or 5-coordinate square pyramidal coordination, where a fifth monodentate co-ligand coordinates in the axial position.[2] In the present study the prospect of using $[Cu_2(\mathbf{5})_2]$ units as a platform, in combination with selected heterocyclic bases as co-ligands, for forming extended structures has been probed.

It is noted that bis(2,4-pentanedionato)copper(II) forms a 1 : 1 adduct with pyridine.[20] Similarly, the interaction of pyridine with $[Cu_2(\mathbf{2})_2]$ has been investigated previously; however, no pure product was obtained in this case due to ready loss of pyridine from the solid complex.[3] In a preliminary experiment, we investigated possible pyridine adduct formation by $[Cu_2(\mathbf{5})_2(THF)_2]$. This complex was recrystallised from a THF/pyridine mixture and the low temperature X-ray structure of the product was obtained immediately after isolation (Fig. 4). The product is of type $[Cu_2(\mathbf{5})_2(py)_2]\cdot py$ (and again rapidly loses pyridine on standing in air). Its structure is similar to that of the starting complex but with pyridine ligands replacing the bound THF molecules. In fact, the molecular (C_i) and space group ($P\bar{1}$) symmetries are the same for these two complexes. Interestingly the pyridine-containing complex crystallised with slightly larger unit cell parameters (details available in Table 2) and, as indicated above, a pyridine solvate molecule is also present.

The tendency of copper(II) in these complexes towards five-coordination was further exemplified by recrystallisation of $[Cu_2(\mathbf{5})_2(THF)_2]$ in the presence of the stronger base, 4-dimethylaminopyridine (dmapy). Crystals of type $[Cu_2(\mathbf{5})_2(dmapy)_2]\cdot 3.25THF$ were obtained and the structure of this product (see Fig. S1 in the ESI†) was shown to be quite similar to that observed for the THF and pyridine analogues described above. The 4-dimethylaminopyridine ligands again occupy the apical positions of the square pyramidal copper(II) centres.

Extended architectures incorporating $Cu_2(\mathbf{5})_2$ units. The preference of the copper(II) complexes for five-coordinate metal centres appeared to provide an ideal avenue for the generation of extended metallo-supramolecular architectures through use of appropriate difunctional heterocyclic bases as co-ligands. Even so, the interaction of $[Cu_2(\mathbf{5})_2(THF)_2]$ with excess 4,4′-bipyridine failed to result in the formation of a bridged extended structure. Instead, a discrete product of type $[Cu_2(\mathbf{5})_2(bipy)_2]\cdot 2bipy$ (Fig. 5) was obtained that has the same stoichiometry, connectivity and general stereochemistry as the analogous dinuclear complexes incorporating the monofunctional ligands THF, pyridine and 4-dimethylaminopyridine. Apart from possible crystal packing effects, we are not able to comment on the reason for 4,4′-bipyridine acting as a (non-bridging) monodentate ligand in this case.

When 4,4′-*trans*-azopyridine was employed as the potential difunctional ligand in place of 4,4′-bipyridine, a one dimensional coordination polymer of stoichiometry $[Cu_2(\mathbf{5})_2(azpy)]_n\cdot(2THF)_n$ was obtained (Fig. 7). An ORTEP representation of the asymmetric unit is provided in the ESI† (Fig. S2). The copper(II) centres are again five-coordinate and approximately square pyramidal, with 4,4′-*trans*-azopyridine ligands occupying apical positions such that they bridge adjacent copper(II) dimer units in a step-like fashion. The resulting arrangement resembles a continuous version of the discrete copper(II) dimer structures discussed above.

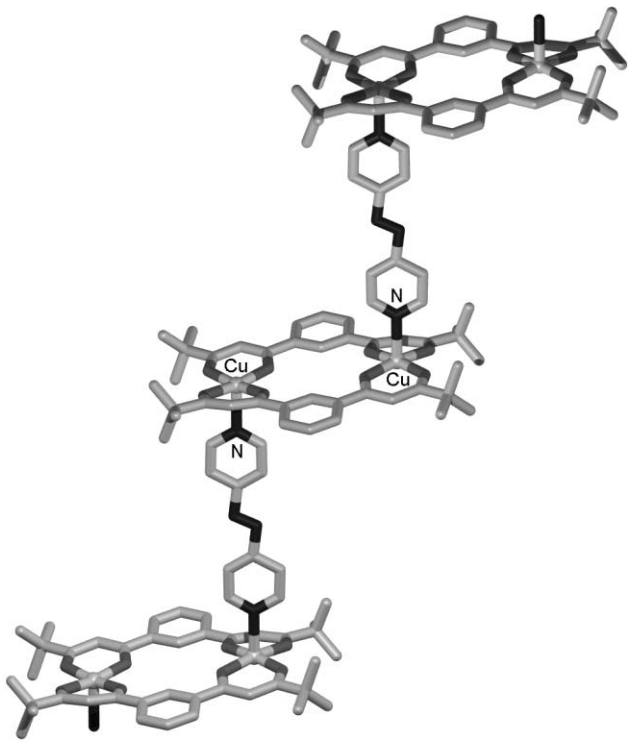

Fig. 7 Portion of the one dimensional polymer chain structure of $[Cu_2(\mathbf{5})_2(azpy)]_n\cdot(2THF)_n$. The step-like structural arrangement consists of dinuclear copper(II) complexes bridged by 4,4′-*trans*-azopyridine ligands (H atoms omitted); the $Cu_2(\mathbf{5})_2$ building blocks of the chain have crystallographic inversion symmetry.

In contrast to the above, interaction of excess pyrazine with $[Cu_2(\mathbf{5})_2(THF)_2]$ yielded the discrete tetranuclear complex $[Cu_4(\mathbf{5})_4(pyz)_2]\cdot 4THF$ whose X-ray structure is illustrated in Fig. 6. As for all of the heterocyclic base-containing complexes discussed so far, the copper(II) centres in this structure are again five-coordinate, with approximately square pyramidal geometries. However, in contrast to the previous structures, the pyrazine ligands protrude on the same side of the mean plane of each dinuclear copper(II) entity such that bridging between copper centres on adjacent complexes takes place to produce a discrete tetranuclear 'dimer of dimers'.

Concluding remarks

The present study reports the complexation of **2**–**5** with copper(II) to yield dinuclear, 'platform-like' complexes as well as dinuclear, triple helical complexes of **2** and **5** with iron(III). Unlike the latter species which incorporate coordinately saturated iron centres, the copper complexes contain coordinately unsaturated metal centres. The present study serves to illustrate the manner by which the latter property may be exploited, through reaction with appropriate N-donor bridging ligands, to yield unusual expanded metallo-assemblies that include both discrete and polymeric structural arrangements.

Acknowledgements

We thank the Australian Research Council for support.

References

1 (*a*) L. F. Lindoy, I. M. Atkinson, *Self-Assembly in Supramolecular Systems, Monographs in Supramolecular Chemistry*, Royal Society of Chemistry, Cambridge, UK, 2000; (*b*) R. M. Yeh, A. V. Davis, and K. N. Raymond, in *Comprehensive Coordination Chemistry II*, ed. J. A. McClevety, T. J. Meyer, Elsevier, Oxford, UK, 2004, vol. 7, pp. 327-355.
2 J. K. Clegg, L. F. Lindoy, B. Moubaraki, K. S. Murray and J. C. McMurtrie, *Dalton Trans.*, 2004, 2417.
3 D. E. Fenton, C. M. Regan, U. Casellato, P. A. Vigato and M. Vivaldi, *Inorg. Chim. Acta*, 1982, **58**, 83.
4 M. M. Matsushita, T. Yasuda, R. Kawana, T. Kawai and T. Iyoda, *Chem. Lett.*, 2000, 812.
5 V. A. Grillo, E. J. Seddon, C. M. Grant, G. Aromi, J. C. Bollinger, K. Folting and G. Christou, *Chem. Commun.*, 1997, 1561.
6 A. P. Bassett, S. W. Magennis, P. B. Glover, D. J. Lewis, N. Spencer, S. Parsons, R. M. Williams, L. De Cola and Z. Pikramenou, *J. Am. Chem. Soc.*, 2004, **126**, 9413.
7 (*a*) D. E. Fenton, J. R. Tate, U. Casellato, S. Tamburini, P. A. Vigato and M. Vivaldi, *Inorg. Chim. Acta*, 1984, **83**, 23; (*b*) T. Shiga, M. Ohba and H. Okawa, *Inorg. Chem.*, 2004, **43**, 4435; (*c*) G. Aromí, P. C. Berzal, P. Gamez, O. Roubeau, H. Kooijman, A. L. Spek, W. L. Driessen and J. Reedijk, *Angew. Chem., Int. Ed.*, 2004, **40**, 18.
8 (*a*) D. Martin, M. Shamma and W. Fernelius, *J. Am. Chem. Soc.*, 1958, **80**, 4891; (*b*) D. J. Gosciniak and N. J. Patrick, *Ultraviolet Radiation Absorbing Compositions of bis-1,3-Diketone Derivatives of Benzene*, 1990, European Patent Application: EP 0 376 511 A2.
9 (*a*) Bruker; *SMART, SAINT and XPREP: Area Detector Control and Data Integration and Reduction Software*. Bruker Analytical X-Ray Instruments Inc. Madison, Wisconsin, USA, 1995; Bruker; *GEMINI: Autoindexing Program for Twinned Crystals*. Bruker Analytical X-Ray Instruments Inc. Madison, Wisconsin, USA, 1999.
10 WinGX-32: System of programs for solving, refining and analysing single crystal X-ray diffraction data for small molecules, L. J. Farrugia, *J. Appl. Crystallogr.*, 1999, **32**, 837.
11 G. M. Sheldrick, *SADABS: Empirical Absorption and Correction Software*. University of Göttingen, Institt fr Anorganische Chemie der Universität, Tammanstrasse 4, D-3400 Göttingen, Germany, 1999.
12 A. Altomare, M. C. Burla, M. Camalli, G. L. Cascarano, C. Giocavazzo, A. Guagliardi, A. G. C. Moliterni, G. Polidori and S. Spagna, *J. Appl. Crystallogr.*, 1999, **32**, 115.
13 G. M. Sheldrick, *SHELX-97: Programs for Crystal Structure Analysis*, University of Göttingen, Institt fr Anorganische Chemie der Universität, Tammanstrasse 4, D-3400 Göttingen, Germany, 1998.
14 L. J. Farrugia, *J. Appl. Crystallogr.*, 1999, **30**, 565.

15 (*a*) R. S. Rasmussen, D. D. Tunnicliff and R. R. Brittain, *J. Am. Chem. Soc.*, 1949, **71**, 1068; (*b*) C. Duval, R. Freymann and J. Lecompte, *Bull. Soc. Chim.*, 1952, **19**, 106.
16 L. L. Funck and T. R. Ortolano, *Inorg. Chem.*, 1968, **7**, 567.
17 (*a*) S. J. Eng, R. J. Motekaitis and A. E. Martell, *Inorg. Chim. Acta*, 1998, **278**, 170; (*b*) M. Morikawa, N. Kimizuka, M. Yoshihara and T. Endo, *Chem. Eur. J.*, 2002, **8**, 5580.
18 A. P. Bassett, S. W. Magennis, P. B. Glover, D. J. Lewis, N. Spencer, S. Parsons, R. M. Williams, L. De Cola and Z. Pikramenou, *J. Am. Chem. Soc.*, 2004, **126**, 9413.
19 R. L. Belford, M. Calvin and G. Belford, *J. Chem. Phys.*, 1957, **26**, 1165.
20 E. Kwiatkowski and J. Trojanowski, *J. Inorg. Nucl. Chem.*, 1976, **38**, 131.